NASA TECHNICAL NOTE

NASA TN D-2441

NASA TN D-2441

SOME OPTICAL TECHNIQUES FOR TEMPERATURE AND CONCENTRATION MEASUREMENTS OF COMBUSTION IN SUPERSONIC STREAMS

by Erwin A. Lezberg and Donald R. Buchele

Lewis Research Center
Cleveland, Ohio

NATIONAL AERONAUTICS AND SPACE ADMINISTRATION • WASHINGTON, D. C. • AUGUST 1964

SOME OPTICAL TECHNIQUES FOR TEMPERATURE AND CONCENTRATION MEASUREMENTS OF COMBUSTION IN SUPERSONIC STREAMS

By Erwin A. Lezberg and Donald R. Buchele

Lewis Research Center
Cleveland, Ohio

NATIONAL AERONAUTICS AND SPACE ADMINISTRATION

For sale by the Office of Technical Services, Department of Commerce,
Washington, D.C. 20230 -- Price $0.75

SOME OPTICAL TECHNIQUES FOR TEMPERATURE AND CONCENTRATION MEASUREMENTS OF COMBUSTION IN SUPERSONIC STREAMS

by Erwin A. Lezberg and Donald R. Buchele

Lewis Research Center

SUMMARY

Three optical techniques are discussed for determining temperature and species concentration in supersonic streams of combustion products. The three techniques are line-reversal pyrometry, determination of the hydroxyl concentration by spectral line absorption, and determination of carbon dioxide and water concentration by infrared spectral absorptance. The line-reversal technique that uses a locally injected emitter and the hydroxyl radical-absorption technique are illustrated by measurements in a supersonic nozzle. The determination of the infrared emitting species has had some limited demonstration in a shock tube. The limitations of these techniques for measurements in exhaust nozzles and supersonic combustion experiments are examined with reference to temperature, optical depth, and response time.

INTRODUCTION

The parameters of most interest in combustion are the gas kinetic temperature and the species concentrations, either their average values or distribution across the stream. These measurements are especially difficult in high enthalpy supersonic flows because of the severe environment and the short testing times dictated by pulse facilities. Gross measurements of performance, such as thrust or pressures, offer little help in understanding chemical kinetic effects on combustion and nozzle flow or in separating these effects from other loss mechanisms.

Conventional techniques of measuring total temperature and major species concentrations that use probes are generally not applicable. Thermocouple materials melt, and the disturbance of the stream or sample by the probe changes the gas composition so that it is no longer typical of the free stream.

Gas sampling for major constituents has been used to a limited extent in investigations of nozzle performance and supersonic combustion (refs. 1 and 2), but the influence of the probe and radical recombination within the probe are somewhat uncertain.

Spectroscopic techniques are not as severely limited with respect to temperature and response time and usually will not disturb the flow. Other limitations are introduced, however, since measurements of radiance and absorptance are usually temporal or spatial averages along the light path. The radiance measurements do not correspond to average temperatures because of the nonlinear relation between radiation and temperature. The methods of spectroscopic pyrometry are well known and are described in recent survey articles (refs. 3 and 4).

Some methods for determining profiles are discussed in reference 4. These methods depend on making multiple measurements either with varying path length through the absorber or varying wavelength. The variation of absorption coefficient with wavelength must be known. The determination of the profile involves the numerical solution of a set of equations for different path lengths or wavelengths and is applicable to systems of simple geometry (e.g., axisymmetric profiles).

This paper will discuss the application of three optical techniques which appear to be suitable for temperature and concentration measurements in supersonic streams of combustion products. These three techniques are spectral line-reversal pyrometry, spectral line absorption in the ultraviolet region for determination of hydroxyl (OH) radical concentration, and spectral absorption in the infrared region for determination of water (H_2O) and carbon dioxide (CO_2) concentration. The latter two methods can also be used to determine a rotational or vibrational temperature. All three methods have been demonstrated to a limited extent in supersonic nozzles or shock tubes (refs. 5 to 10).

SYMBOLS

A_K relative transition probability

a broadening parameter, $\frac{(b_N + b_C)(\ln 2)^{1/2}}{b_d}$

B constant in eq. (2)

b_C collision half-width, cm^{-1}

b_D Doppler half-width, cm^{-1}

b_N natural half-width, cm^{-1}

C_2 Planck's second radiation constant

c speed of light, cm/sec

d line spacing, cm^{-1}

e electron charge

erfc	error function
exp	exponential
F	defined by eq. (5)
f	ratio of number of dispersion electrons to number of absorbers
h	Planck's constant
I	relative source intensity
J	rotational quantum number
k	Boltzmann's constant
k	constant in eq. (2)
l	path length, cm
m	electron mass
N_λ	radiant intensity
N	number density, cm^{-3}
P	absorption coefficient, cm^{-1}
P'	absorption coefficient at center of Doppler broadened line, cm^{-1}
p	pressure, atm
Q_R	rotational partition function
Q_V	vibrational partition function
q	dynamic pressure
S^o/d	line strength parameter, $(atm^{-1})(cm^{-1})$
T	temperature
$\overline{T}$	average temperature
$T_{J'J''}$	correction factor to transition probabilities for vibration-rotation interaction
W	equivalent width, cm^{-1}
$\alpha(\lambda)$	absorptance, $1 - I/I_o$
γ^o/d	half-width parameter, atm^{-1}

ϵ emissivity

λ wavelength

τ fractional transmittance, I/I_o

φ equivalence ratio

ω wave number, cm^{-1}

Subscripts:

A air

a absorbing gas

b broadening gas

d spectral line

g gas

J rotational quantum number

K rotational level

o initial

s reference source

v optical pyrometer

λ wavelength

ω wave number

ω_o wave number at center of spectral line

Superscripts:

' upper state

" lower state

SPECTRAL LINE REVERSAL

Description of Method

The use of the line-reversal technique for temperature measurements has been treated extensively (refs. 3, 10, and 11). A self-balancing reversal pyrometer has been described (ref. 11) and is shown schematically in figure 1.

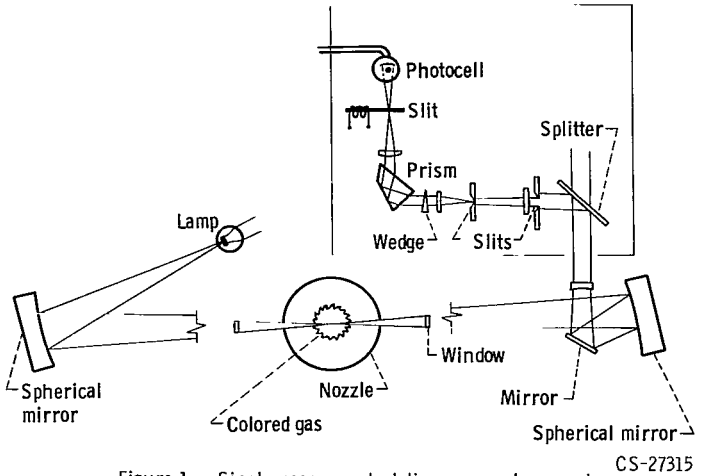

Figure 1. - Single-pass, spectral-line-reversal pyrometer.

The instrument uses either a tungsten ribbon lamp or a carbon arc as a comparison source. Local temperature measurements can be obtained in high-velocity gas streams by the injection of a spectrally radiating compound into the gas through a probe. The method requires equal intensities $N_{\lambda,g}$ and $N_{\lambda,s}$ of blackbodies at gas and reference source temperature, respectively. The reversal equation for the instrument used as a single-pass system in figure 1 is

$$N_{\lambda,g} = (\tau\epsilon_{\lambda,s}N_{\lambda,s})\tau' \qquad (1)$$

where τ is the fractional transmittance of the optics between the source and the gas, $\epsilon_{\lambda,s}$ is the source emissivity, and τ' is a correction factor for gas radiation reflected from the source and intervening optics. The term $\tau\epsilon_{\lambda,s}N_{\lambda,s}$ is obtained as a temperature by calibration with an optical pyrometer. The temperature is corrected for the wavelength shift from λ_v of the optical pyrometer to λ_d of the spectral line. The calibration and instrument errors are described in reference 11.

The temperature of sodium when used as a spectral emitter has been identified with the vibrational temperature of the gas (ref. 12), and its use for determining kinetic temperature requires at least equilibration of vibration with the translational and rotational modes. The temperature limits for the line-reversal pyrometer are determined by the lower limit at which the emitter produces sufficient intensity to produce a usable signal at the detector and an upper limit at which the maximum source temperature is reduced by the source emissivity $\epsilon_{\lambda,s}$ and transmission τ of the intervening optics. The limits for the instrument described herein in which sodium is used as a tracer are estimated to be 1500° to 3280° K, when a carbon-arc source and refracting optics that are multilayer coated for low reflectance are used.

Experimental Measurements

Experimental temperature measurements have been obtained in supersonic nozzles for hydrogen-air and methane-air combustion products. These measurements are described in detail in reference 5. The self-balancing spectral line-reversal pyrometer described in the preceding section was used both as a single- and a double-pass instrument. The spectral lines used were the sodium doublet at 5893 angstroms and the blue line of cesium at 4553 angstroms. Either sodium carbonate or cesium sulfate were introduced as powders in a carrier gas stream at the exit of the subsonic combustion chamber. The determination of a temperature profile at the combustor exit is illustrated in figure 2. The temperature profile was determined by traversing a powder injector parallel

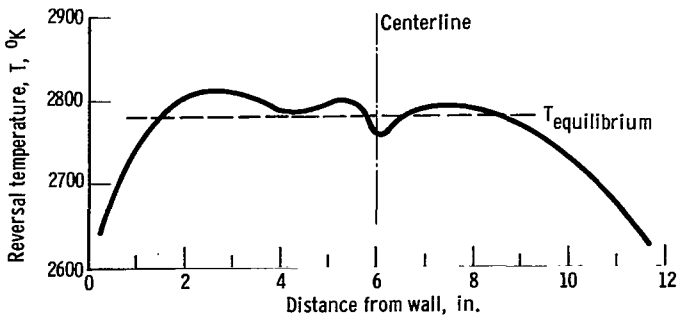

Figure 2. - Combustor temperature profile by traversing powder injector parallel to collimated source beam. Reversal of cesium 4553-angstrom line. Natural gas fuel; initial pressure, 3.6 atmospheres; equivalence ratio, 0.954; air temperature, 1790° K.

to the axis of the collimated source beam. Temperature profiles were not attempted at the optical port locations in the supersonic portion of the nozzle since spreading of the tracer stream would obscure any details of a radial profile. Some typical temperature measurements in the nozzle are shown as a function of equivalence ratio at nozzle-area-to-throat-area ratios of 1.23, 1.60, and 2.02 in figure 3. The dashed curve is for a simplified kinetic calculation in which the Bray freezing point approximation was used (ref. 5). Observations of the yellow D-line light produced by the normal shock at the nozzle exit indicated that sodium was confined to the central core of the jet and that the temperature measurements were not influenced by the colder boundary-layer gas.

Experimental Error

Differences between the self-balancing instrument and a manual instrument had an average random deviation of 20° R (ref. 11). Comparisons of measured temperatures of the line-reversal pyrometer with probe-type pyrometers are

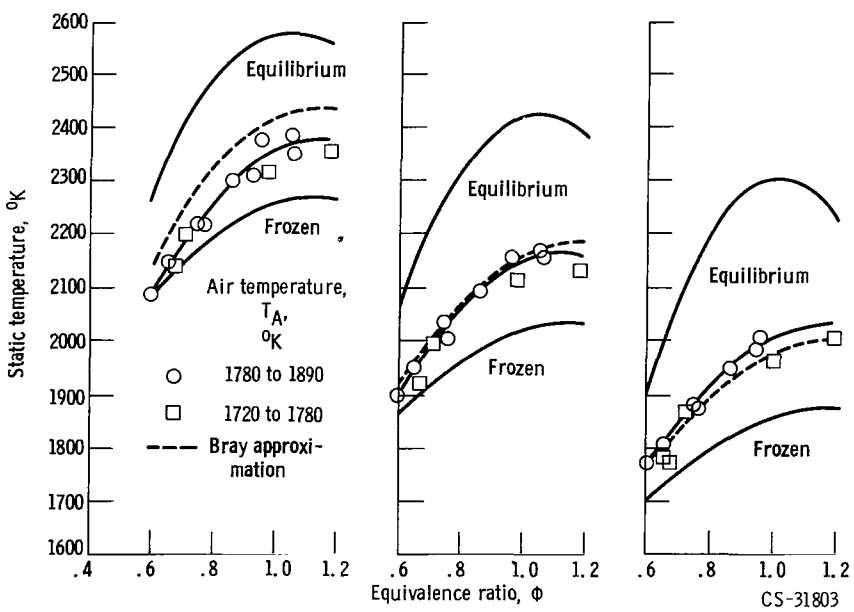

(a) Nozzle area ratio, 1.23. (b) Nozzle area ratio, 1.60. (c) Nozzle area ratio, 2.02.

Figure 3. - Effect of equivalence ratio on nozzle static temperature. Initial pressure, 3.6 atmospheres.

given in reference 13. A discrepancy of a few percent has been partially accounted for as an averaging error due to temperature fluctuations in the combustion tunnel (ref. 14).

The error in measuring the average of a temporal or spatial temperature fluctuation is due to the nonlinearity of radiance with temperature. In spectral regions where the Planck function is steep, the measurements may be much closer to the peak temperature than the average.

The fractional averaging error $(\overline{T} - T_o)/T_o$ is given for small errors as (ref. 14)

$$\frac{\overline{T} - T_o}{T_o} = k\left(\frac{C_2}{\lambda T_o} + \frac{B}{T_o} - 2\right)\left(\frac{\Delta T}{T_o}\right)^2 \tag{2}$$

where $\Delta T/T_o$ is the fractional average deviation of the temperature fluctuations, and B is a constant that accounts for the variation of emitter concentration with temperature determined from equilibrium calculations. The constant k depends on the waveform of the fluctuations and will have values of $k = 0.62$ for a sinusoid, $k = 0.79$ for a random wave, and $k = 0.5$ for a square wave. The error due to temporal and spatial fluctuations can be determined by flux measurements and related to the temperature fluctuation (when it is small) by

$$\frac{\Delta T}{T_o} = \frac{T_o}{\frac{C_2}{\lambda} + B} \frac{\Delta(N_\lambda P_\lambda)}{N_\lambda P_\lambda} \tag{3}$$

where $N_\lambda P_\lambda$ is the average radiation, and $\Delta(N_\lambda P_\lambda)$ the average deviation of the fluctuations. Substituting the temperature fluctuation in equation (2) yields the averaging error in terms of radiance fluctuations.

The error in the reversal temperature due to temperature fluctuations in the gas was determined by radiant flux measurements at a nozzle-area ratio of 1.60 and fuel-air equivalence ratio of 0.9. Radiation from the OH radical, ultraviolet bands at 3070 angstroms, was focused on the entrance slit of a 0.5-meter grating monochromator with photomultiplier detector. The exit slit was removed to obtain sufficient intensity for the measurements and, therefore, included the entire 0-0 band. The signals from chopped and unchopped radiation were used, respectively, to determine the temperature fluctuation and fractional averaging error from equations (2) and (3). The fluctuations were found to be approximately 5° K at a static temperature of 2100° K; the averaging error was entirely negligible.

SPECTRAL LINE ABSORPTION FOR THE HYDROXYL RADICAL

Discussion of Method

The concentration of the OH radical can be determined by absorption in the

ultraviolet $^2\Sigma^+ - {}^2\Pi$ electronic band (ref. 15).

The method used is that of reference 16 in which the light source is a low-pressure discharge in water vapor thus producing the OH emission spectrum. The emission line in the source is absorbed by the broader Doppler-shaped line of the gas so that ideally only absorption at the line center is measured. The absorption at the line center is related to the ground-electronic-state population by the f number for the transition and the shape of the absorbing line. The f number is defined as the ratio of the number of dispersion electrons to the number of absorbers and is related to the electronic transition probability. The f number has been experimentally determined by measuring the integrated absorption of a number of lines in the 3064-angstrom 0-0 band and relating the absorption to the known concentration of OH in the absorbing gas (refs. 15 and 17 to 19). Since the OH concentration must be calculated from its thermodynamic properties, changes in the accepted value for the heat of formation of OH will change the value of the f number.

From the definition of the f number, the number density of OH in the lower rotational level J'' is

$$N_{J''} = \frac{mc^2}{\pi e^2 f} \int_{-\infty}^{\infty} P_\omega d\omega \tag{4}$$

where P_ω is the absorption coefficient per centimeter of path length at the wave number ω.

The f number has been given in reference 16 as

$$f = \frac{FA_K}{2J'' + 1} \tag{5}$$

where A_K is the relative transition probability tabulated in reference 20 for the OH rotational levels. Recently the vibration rotation interaction has been calculated for the P, Q, and R branches of the $^2\Sigma^+ - {}^2\Pi$ transition (ref. 21). Inclusion of this effect will change the transition probabilities since Dieke and Crosswhite assumed that the rotational and vibrational transition probabilities were completely separable (ref. 20). The resultant correction factors cause a variation of the electronic transition probabilities with rotational quantum number so that F in equation (5) cannot be taken as a constant.

For a line with Doppler shape

$$\int_{-\infty}^{\infty} P_\omega d\omega = b_D P' \left(\frac{\ln 2}{\pi}\right)^{-1/2} \tag{6}$$

where P' is the absorption coefficient of the Doppler broadened line at the line center, and b_D is the Doppler half-width in centimeters^{-1}.

The line shape for a combination of Doppler and collision broadening can be written in terms of the broadening parameter a:

$$a = \frac{(b_N + b_C)(\ln 2)^{1/2}}{b_D} \tag{7}$$

where b_N and b_C are the natural and collisional half-widths. The value of a has been assumed equal to zero (ref. 16), although other values of a have been indicated (refs. 17 and 22). For other values of a the relation between the absorption coefficient at the line center and the Doppler coefficient is given in reference 23 as

$$P_{\omega_o} = P' \left[\exp(a^2)\right] \left[\operatorname{erfc}(a)\right] \tag{8}$$

where P_{ω_o} is the absorption coefficient at the line center. Numerical values of P_ω/P' are given in table 4-3 of reference 23. The measured absorption coefficients can then be corrected for collisional broadening in the gas if the value of a is known.

For rotational equilibrium, the total concentration of OH in the ground $^2\Pi$ state is

$$N_{OH} = N_{J''} \frac{Q_R Q_V}{2J'' + 1} \exp\left(\frac{hc\omega_K}{kT}\right) \tag{9}$$

where Q_R and Q_V are the rotation and vibration partition functions and ω_K the rotational energy level in centimeters^{-1}.

Combining equations (4), (5), (6), and (9) and inserting the numerical values for the constants give

$$N_{OH} = \frac{Q_R Q_V b_D P'}{f A_K T_{J'J''}} \exp\left(\frac{hc\omega_K}{kT}\right) \times 2.40 \times 10^{12} \tag{10}$$

where $T_{J'J''}$ is the correction factor for vibration rotation interaction given in reference 21. Recently, two new determinations of the f number have been reported (refs. 24 and 25). Neither depends on thermochemical data, and one (ref. 24) represents a direct determination of the radiative lifetime of the $^2\Sigma^+ - {}^2\Pi$ transition of OH. These investigations indicate a band oscillator strength, $f_{0-0} = 8 \times 10^{-4}$ ±10 to 15 percent or a value of $F = 2.0 \times 10^{-4}$. This value has been used in equation (10), rather than one of the earlier values, because of the lower error estimate and the fact that the newer determinations are independent of thermochemical data.

Experimental Measurements

The experimental apparatus is shown schematically in figure 4. The facility and external optical arrangement is essentially the same as the line-reversal instrument. The light source used was an end-view capillary discharge tube (fig. 5). Water-vapor pressure was maintained at 0.8 to 1.0 millimeter of mercury by pumping on a sulfuric acid solution connected to the lamp and kept at 0° C in an ice bath. A current of 40 milliamperes drawn from a 5000-volt

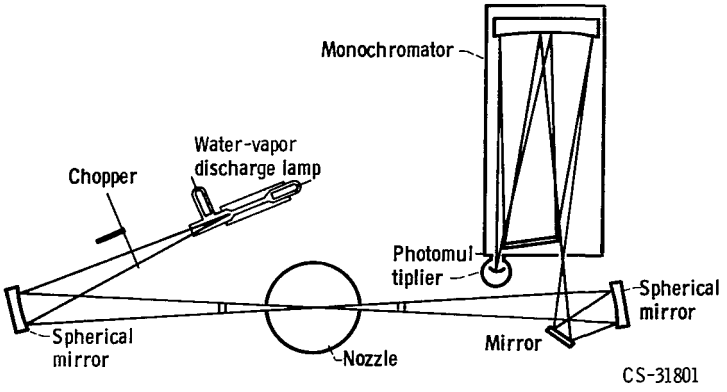

Figure 4. - Optical arrangement for line-absorption measurements.

transformer was used during this series of measurements. Light from the source was chopped at 120 cps and focused at the center of the nozzle. The emerging beam was refocused at the entrance slit of a 0.5-meter Ebert-mount grating monochromator equipped with a photomultiplier detector.

The absorption measurements were made by scanning the spectrum of the lamp with a nonabsorbing gas (air) flowing through the nozzle and with the absorbing gas (hydrogen-air combustion products) in the light path. Since the light was chopped on the source side, and only the chopped signal was amplified, possible emission from the gas was not recorded.

Mole fraction of OH was calculated by using equation (10), the measured absorption, the static pressure, and the reversal temperature. Results are shown as a function of the fuel-air equivalence ratio in figure 6. Data are shown at nozzle area ratios of 2.02 and 2.49 at a combustor stagnation pressure of 3.6 atmospheres. The absorption measurements were made in this case by scanning past the spectral line at each fuel setting. The equilibrium mole fractions of OH were computed from the IBM 7090 program of reference 26. The upper curve was computed by assuming that the OH mole fraction froze at the nozzle throat. The hydroxyl radical is not expected to be completely frozen at these nozzle area ratios because of the continuing bimolecular shuffle reactions (ref. 27).

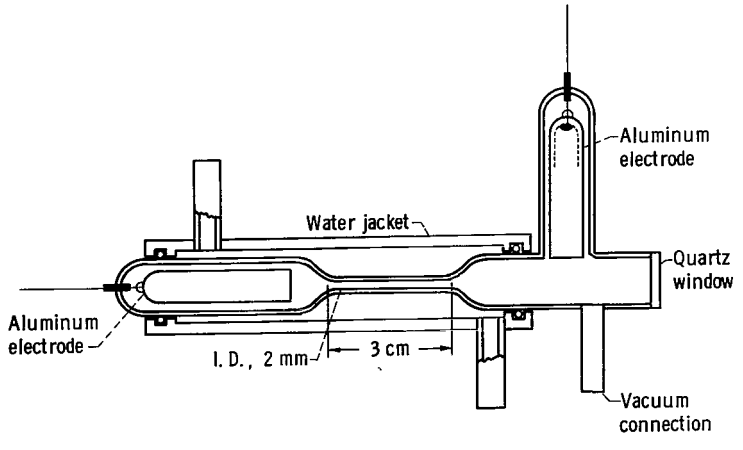

Figure 5. - End-view discharge tube.

Experimental Errors

Checks of rotational equilibrium were made by scanning a portion of the spectrum and determining the absorption coefficient $P_{\omega_o} = \ln I_o/I$ for a number of lines in the 0-0 band. The rotational temperature can be determined by plotting $\log P_{\omega_o}/A_K T_{J',J''}$ against the rotational energy of the transition and taking the slope of the resulting straight line. Within experimental error, the lines were straight and the temperature was generally within 100° K of the measured reversal temperature. Slight dirtying of the test section windows during the run caused much larger departures of the apparent rotational temperature from the reversal temperature. In addition to

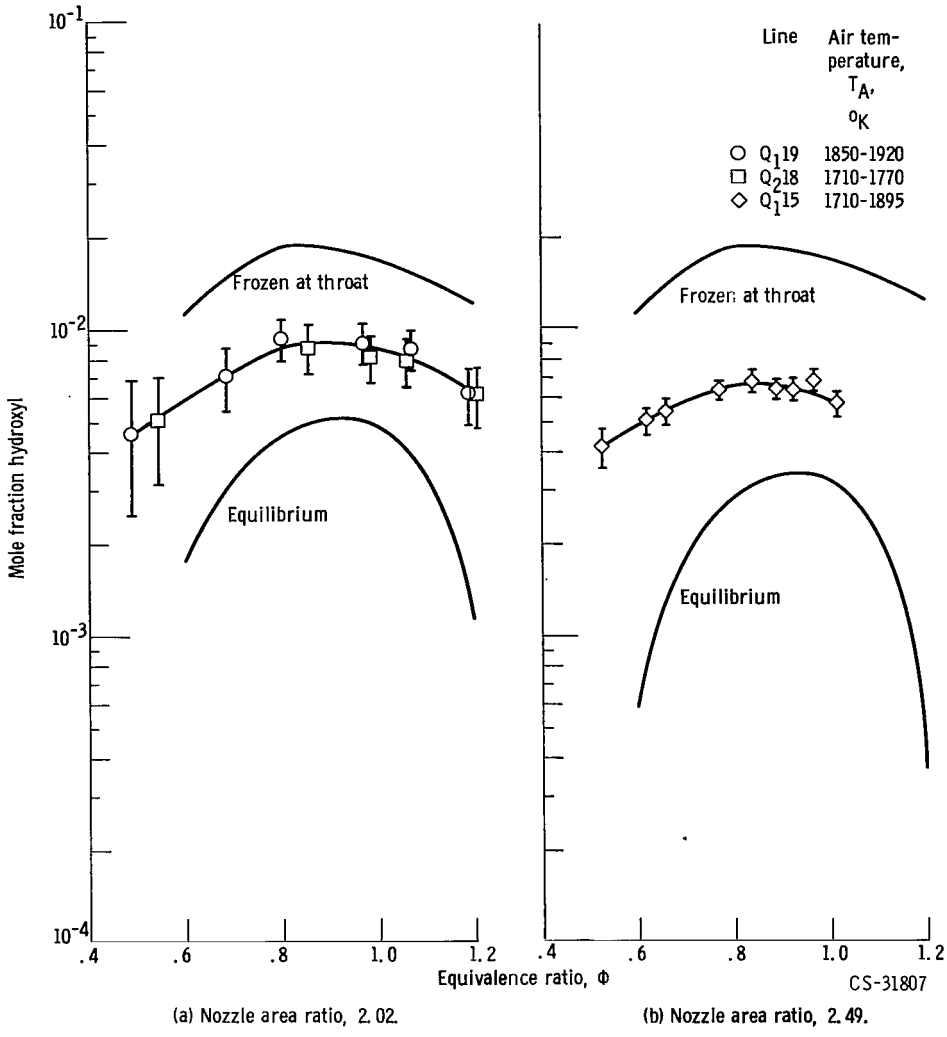

Figure 6. - Hydroxyl concentration by line absorption of $^2\Sigma^+ - {}^2\Pi$ transition, 0-0 vibrational band, hydrogen-air combustion products. Initial pressure, 3.6 atmospheres.

the change in I_o, the determination of the rotational temperature involved absorption measurements of some stronger lines that were 90 percent or more absorbed and, therefore, subject to errors due to self-absorption.

The experimental error in measuring the absorption coefficient $P\omega_o$ due to changes in source intensity I_o was estimated and is indicated by the length of the data bars in figure 6. Changes in I_o could occur through slight dirtying of the test section windows, through changes in source current or pressure, or through the movement of the source image with respect to the entrance slit due to vibration or refraction of the light by density gradients in the test gas. The change in the source intensity was usually less than 5 percent. The low-frequency noise level of the source was about 3 percent. Errors in the reversal-temperature measurement could result in concentration errors due to the temperature effect on the population distribution, the half-width, and the

gas density. A 5 percent error in the reversal temperature would result in a 4 percent error in the OH mole fraction for the $Q_1 15$ line at 1850° K.

In addition to uncertainties in the f value noted previously, errors due to lack of knowledge of the line shapes and widths in the discharge lamp and gas should be considered. Since the source line width is not infinitesimally small, a correction can be applied for its finite width. If it is assumed that both the source and the absorption lines are Doppler broadened, the ratio of source to absorption line widths can be given by the square root of the absolute-temperature ratio. The error in the absorption coefficient P' and hence in the calculated mole fraction due to source line width can be calculated from the tabulated values of reference 28.

For combined collision and Doppler-broadened lines in the absorbing gas, the error in the absorption coefficient can be calculated from equations (7) and (8), or the tabular values of reference 23. If collision broadening in the absorber is significant, the error due to finite source width would be correspondingly diminished.

The total correction to the mole fractions of OH shown in figure 6 can be estimated for the line-shape corrections, which appear to be the best values available at the present time. The corrections would include an absorber-line-shape parameter, a = 0.05 (ref. 17), and a source-line width equal to half the absorber width. The total correction would increase the values of the mole fractions by a factor of 1.18 with an uncertainty of approximately 30 percent.

INFRARED SPECTRAL ABSORPTION

Discussion of Method

Concentration of infrared absorbing species such as CO_2 and H_2O can be determined by spectral absorption at the band wavelengths of 4.3 and 2.7 microns, respectively. Concentration measurements of CO_2 and H_2O in a supersonic nozzle have not been reported, although Ferrisso (ref. 6), has made emission-absorption temperature measurements at the exit of a small rocket nozzle by using the 4.3-micron CO_2 bands and the 2.7-micron water-vapor bands. Absorption coefficients of CO_2 were determined at the nozzle exit and related to concentrations with a thermochemical calculation based on a sudden freezing approximation.

In situ measurements are possible by a comparison of the experimental absorptance with the absorptance measured at the same wavelength for a series of calibration experiments (ref. 29). The calibration measurements are, in general, required at each temperature and optical path length. Clearly, this method begins to get out of hand when a wide range of experimental conditions is encountered.

With CO_2, it has been found that absorption generally does not follow the simple Lambert-Beers law (refs. 29 and 30) so that extrapolation of data is unsatisfactory. Recently, Oppenheim (ref. 30) has shown that the statistical band model of Plass (ref. 31) can be applied to the 4.3-micron CO_2 bands at

1273° K by using the "curve of growth" method. Absorption of CO_2 is represented as a unique function of the statistical band parameters over a wide range of pressures and optical depths. The curve of growth represents the "growth" of the integrated absorptance W as the number of absorbers in the optical path increases. The work of reference 9, which has been supported by the NASA Lewis Research Center, has extended the use of the statistical model to the 2.7-micron water-vapor bands and has included the effects of foreign gas broadening.

The statistical model relates the absorption parameter, $\ln(1/\tau)$, to absorber partial pressure and path length:

$$\ln \frac{1}{\tau} = 2\pi \frac{\gamma^o}{d} p_a f(x) \tag{11}$$

where

$$f(x) = xe^{-x}\left[J_0(ix) - iJ_1(ix)\right] \tag{12}$$

and J_0 and J_1 are Bessel functions with imaginary arguments. The parameter

$$x = \frac{\frac{S^o}{d} p_a l}{2\pi \frac{\gamma^o}{d} p_a} \tag{13}$$

where S^o/d is the line strength parameter, γ^o/d the half-width parameter, and d the line spacing.

The effect of foreign gas broadening can be included by writing the dimensionless half-width in terms of the partial pressures of absorber and broadener:

$$\frac{\gamma^o}{d} = \frac{\gamma_a^o}{d} + \frac{p_b}{p_a} \frac{\gamma_b^o}{d} \tag{14}$$

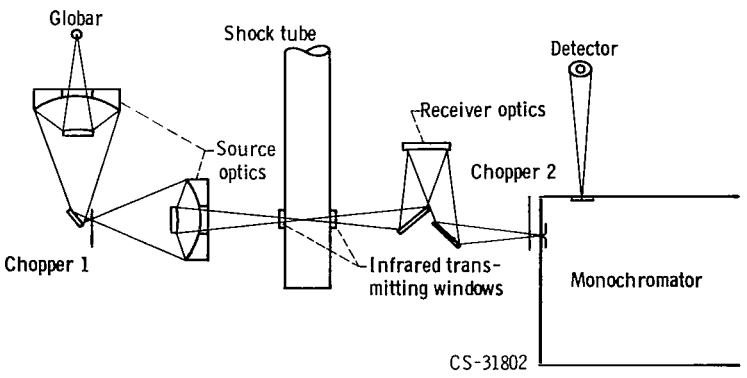

Figure 7. - Schematic diagram of infrared absorption optics for shock tube.

Experimental Measurements

Absorption measurements (ref. 9) were made for CO_2 mixture at 4.40 microns in electrically heated gas cells, flat-flame burners, and shock tubes. Similar measurements were made for H_2O mixtures at 2.506 and 2.854 microns. A schematic drawing of the experimental apparatus used with the shock tube is shown in figure 7. The light source is a

globar, the detector is a vacuum thermocouple, a lead sulfide cell, or a liquid-nitrogen-cooled indium antimonide cell. The use of two choppers permits simultaneous absorption-emission measurements, from which the temperature can be determined (ref. 29). For the shock tube experiment the emission and absorption are measured simultaneously by using direct- and alternating-current electronics in parallel. Chopper 1 was driven by an air turbine that gave a chopping rate of 80 kilocycles.

Water-vapor-absorption measurements require the optical path to be purged with nitrogen to minimize atmospheric absorption. Initial measurements with a prism instrument gave measured absorptances of 0.10 or less for the optical depths investigated. With the prism resolution of 18 centimeter^{-1}, the absorptance was decreased because of the averaging of the spaces between the H_2O rotational lines. When the Litrow mirror in the monochromator was replaced with a grating, the spectral resolution was increased to 2 centimeter^{-1}, and a spectral region could be chosen to include a few strong lines. The increase in absorptance resulted in a decrease in errors in the absorptance measurements.

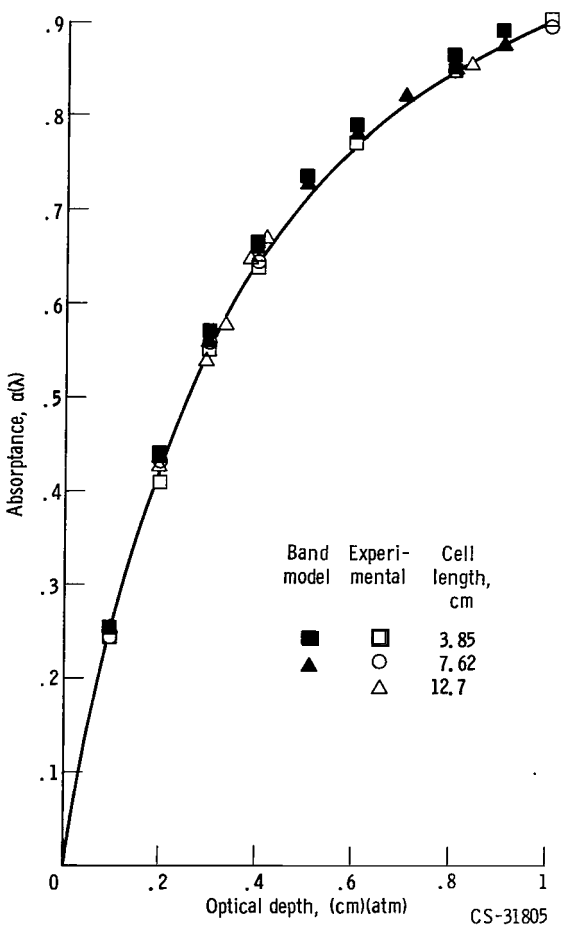

Figure 8. - Comparison of experimental data and band-model prediction for carbon dioxide - nitrogen mixtures (ref. 9). Temperature, 1273^{0} K; wavelength, 4.40 microns; pressure, 700 millimeters of mercury.

Furnace and shock tube measurements of absorptance of CO_2 and CO_2-nitrogen mixtures were made from 600^{0} to 2400^{0} K at 4.40 microns to determine the strength parameter S^{0}/d. The half-width parameter γ^{0}/d was determined only to 1273^{0} K. From the values of S^{0}/d and γ^{0}/d at 1273^{0} K, the absorptance was calculated by using equation (11) and compared with experimental measurements (fig. 8). Agreement of shock tube measurements at 2000^{0} to 2300^{0} K was within 1 to 7 percent of the calculated statistical model (ref. 32).

Measurements of water-vapor - nitrogen mixtures were made up to 1273^{0} K by using the nitrogen-purged system. These results are shown for $\lambda = 2.854$ microns in figure 9. A temperature extrapolation of the band-model parameters based on the theoretical behavior of a single line was in poor agreement with flat-flame burner measurements at high temperatures, although good agreement was obtained with furnace data at lower temperatures. Since the distribution of line strength in the bands changes with temperature, further measurements of the band parameters at higher temperatures are required.

APPLICATIONS TO SUPERSONIC-COMBUSTION TESTING

Combustor inlet and exit conditions are given in table I for a range of flight Mach numbers for hydrogen-fueled hypersonic ramjets. At a Mach number of 12, the static temperature and H_2O mole percent is plotted in figure 10 as a function of distance for a small supersonic combustor and nozzle. Mole percent OH is shown in figure 11. The data were taken from the kinetic calculations of reference 27 for a nozzle with a thoat radius of 1 centimeter. These calculations assume instantaneous mixing so that rates of change of temperature and species concentration in the combustor are optimistically fast.

TABLE I. - COMBUSTOR CONDITIONS

Combustor condition	Flight Mach number			
	8	12	20	27.3
Combustor inlet static pressure, atm	5	5	2	1
Combustor inlet static temperature, ^{o}K	1100	1640	2240	2640
Combustor inlet Mach number	2.94	3.93	7.23	8.39
Hydrogen-air equivalence ratio	1	1	2	6
Combustor exit static temperature, ^{o}K	2833	3049	3105	2879
Mole fraction H_2O	0.293	0.256	0.210	0.1155
Mole fraction OH	0.0206	0.0350	0.0250	0.00555

Temperature Measurements

It can be noted from table I that the range of combustor inlet and exit temperatures is generally within the range of the reversal-temperature technique. It appears also that the rate of temperature rise for the case illustrated (fig. 10) can be followed along the combustor. Since the rate of average temperature rise will be mixing-limited under at least some of the flight conditions given in table I, it should be possible to use a locally injected tracer to follow the temperature of a stream tube. The practical problem of introducing the spectral emitter remains, but a small probe could introduce a gaseous tracer (e.g., chromium carbonyl, ref. 33) far enough upstream that the effects of the probe on the stream would have dissipated. A limitation might be the minimum concentration of emitter necessary to achieve adequate sensibility for the reversal measurement. The maximum allowable spreading of the tracer stream would depend both on concentration and desired spatial resolution. Facility limitations will probably preclude long duration testing at Mach numbers in excess of 8 and higher flight speed simulation restricted to pulse facilities, such as the shock tunnel, with test times in the millisecond range.

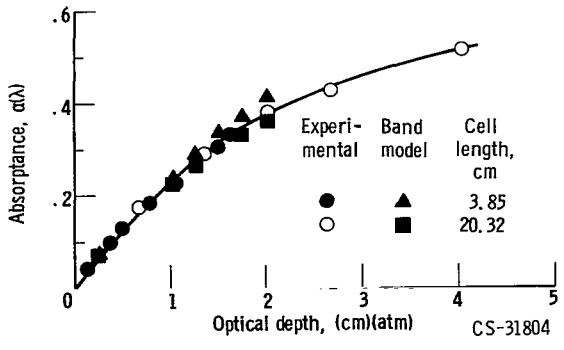

Figure 9. - Comparison of experimental data and band-model prediction for water-nitrogen mixtures (ref. 9). Temperature, 1273° K; wavelength, 2.854 microns (3504 cm^{-1}); pressure, 700 millimeters of mercury.

A double-beam setup for applying the

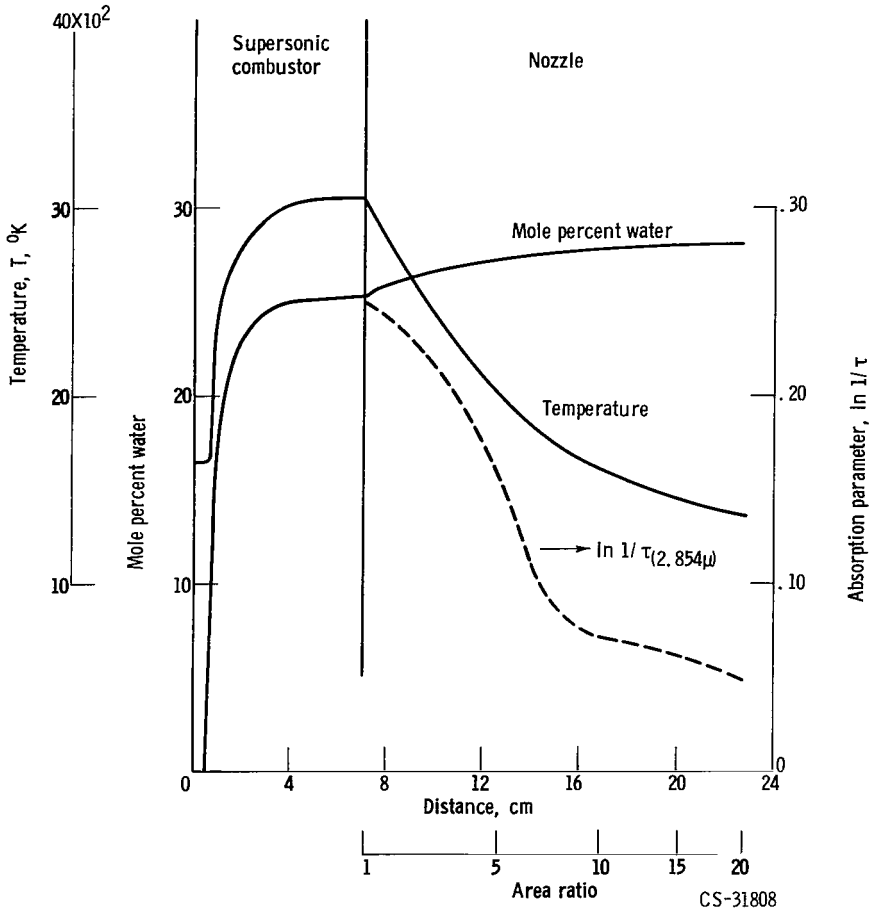

Figure 10. - Water concentration and absorption parameter for kinetic flow in supersonic combustor and nozzle. Free-stream Mach number, 12; initial pressure, 5 atmospheres; equivalence ratio, 1; throat radius, 1 centimeter.

reversal method to a shock tube is given by Gaydon (ref. 12). Another technique has been described (ref. 34) in which the monochromator slit is divided vertically, the source is focused at the top half of the slit, and gas radiation is focused at the bottom half. Light at the exit slit is then focused on two photomultiplier tubes. A third technique might be to chop a high temperature source with a high speed chopper consisting of a slotted disk combined with a series of neutral step filters.

TABLE II. - ABSORPTION PARAMETERS AT COMBUSTOR EXIT

Absorption parameter	Flight Mach number			
	8	12	20	27.3
$(P'l)_{OH}$ $(Q_1 15)$	6.95	11.15	3.22	0.378
$(P'l)_{OH}$ $(Q_1 21)$	1.195	2.20	0.654	0.0659
$\left(\ln \frac{1}{\tau}\right)_{H_2O}$ (2.854 μ)	0.308	0.249	0.0763	0.0246

Hydroxyl-Concentration Measurements

The absorption coefficient has

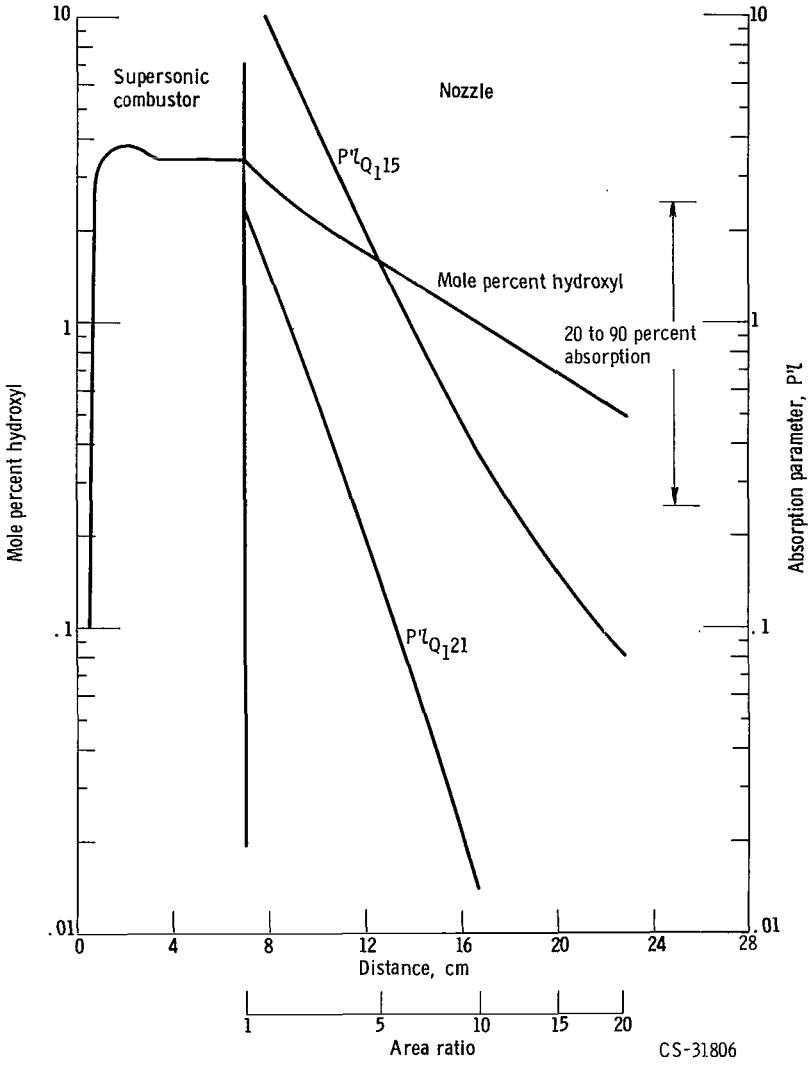

Figure 11. - Hydroxyl concentration and calculated absorption parameter for $Q_1 15, Q_1 21$ rotational lines. Free-stream Mach number, 12; supersonic combustor and nozzle.

been calculated from equation (10) for the combustor exit conditions given in table I and a path length of 2 centimeters; the results are given in table II. Since a usable range of absorption coefficients will be $P'l \simeq 0.22$ to 2.5 (20 to 90 percent absorption at the line center), the rotational line must be chosen to limit the optical depth and, hence, to limit errors due to self-absorption or source fluctuations. The choice of rotational lines is not unduly limited by the source since the low-pressure discharge described previously has nearly equal intense lines for the higher quantum number lines of a particular branch. The $Q_1 21$ line was somewhat arbitrarily chosen as an upper limit in quantum number of the source lines since the error in concentration due to a temperature error increases rapidly for the higher energy levels because of the exponential term in equation (10).

The absorption coefficients as given in table II are seen to be acceptable for the range of optical densities of the given conditions. The combustor static pressures given in table I represent a high flight dynamic pressure (q_o = 5000 lb/sq ft). At a q of 1500 pounds per square foot, which may represent a more reasonable flight trajectory, the static pressures and optical depths would be lower by a factor of 4 to 10, and the experiment could be scaled upward by the same factor for the same range of absorption coefficients. For experiments of larger scale, it may be possible to use other bands such as the 1-1 vibrational transition where the population is about 12 percent of the 0-0 band for the temperatures given. The rate of increase of OH in the combustor is so rapid for the examples given that it would be extremely difficult to follow the ignition reactions except possibly where combustion is mixing-limited. Because of the large exponential

dependence of population on temperature, the change in absorption coefficient would be much steeper than indicated by the mole percent OH. The coefficients multiplied by path length for the $Q_1 21$ and $Q_1 15$ lines are shown plotted as a function of distance in figure 11. It is apparent that any limitations imposed by high optical depths will disappear at the higher area ratios.

Water-Vapor-Concentration Measurements

Since water is a major constituent in hydrogen-air combustion products, it can be used to follow the progress of reaction or mixing. For the example shown in figure 10, it is seen that, following the initial rapid buildup during the ignition reactions, there is a slower increase due to the recombination of the radicals and atoms. In the nozzle, freezing appears to be much more pronounced than for OH. Since the actual change in the nozzle is approximately 10 to 20 percent of the mole fraction initially present at the beginning of the expansion, the restrictions on experimental accuracy in a concentration measurement are more stringent. Experimental difficulties are also aggravated by the need to purge atmospheric water vapor out of the optical path.

The absorption parameter $\ln(1/\tau)$ has been calculated for water vapor for the conditions in table I. The band-model relation of equation (11) was used. The band-model parameters were extrapolated to higher temperatures from the values determined at 1273° K in reference 29. The strength and half-width parameters were assumed to vary with temperature in the same way as a single spectral line (ref. 9):

$$\frac{S^{\circ}(T)}{d} = \frac{S^{\circ}(1273)}{d} \left\{ \exp\left[-2160 \left(\frac{1}{T} - \frac{1}{1273} \right) \right] \right\} \left(\frac{1273}{T} \right)^{5/2} \tag{15}$$

The temperature variation of the total half-width is

$$\frac{(\gamma^{\circ}/d)1273}{(\gamma^{\circ}/d)T} = \left(\frac{T}{1273} \right)^{0.66} \tag{16}$$

Since the actual variation of the strength and width parameters are not available above 1273° K, the usefulness of these expressions remains in doubt. The calculated absorption parameter is shown in table II. It can be seen that, for the scale of this experiment, the determination of H_2O concentration is only feasible at the combustor conditions for the cases of flight Mach number equal to 8 and 12. There is insufficient water present for the other two conditions. For the nozzle expansion at Mach 12 the H_2O concentration is high enough for measurements out to an area ratio of approximately 8 without excessive error. It would appear that, for an experiment where the concentration is to be measured by spectral absorption, the scale of the experiment should be chosen so that absorptance is in a useful range.

SUMMARY OF RESULTS

Three optical techniques for temperature- and species-concentration mea-

surements in supersonic streams have been described. These techniques are as follows:

1. The spectral-line-reversal method for determining static temperatures

2. Line absorption spectroscopy for determination of the hydroxyl radical concentration in which the hydroxyl $^2\Sigma^+ - {}^2\Pi$ electronic transition was used

3. Infrared spectral absorption for determination of carbon dioxide and water concentrations (in which a statistical band model was used to relate spectral absorptance to concentration)

Experimental measurements of reversal temperature (ref. 5) and hydroxyl radical concentration were made in a supersonic nozzle that expanded the combustion products of hydrogen and air. These measurements are presented herein as a demonstration of the optical techniques.

Shock tube and furnace measurements of water and carbon dioxide absorptance in gas mixtures (ref. 9) showed good agreement with a statistical band model that includes the effects of spectral line broadening by other components of the mixture.

Errors due to temporal or spatial temperature fluctuations, instrumental errors, and errors in knowledge of transition probabilities or band-model parameters were considered.

The application of these optical techniques to supersonic combustion experiments is discussed, and some of the limitations are estimated. The range of temperatures for the reversal technique in which a carbon arc source and a sodium tracer were used is 1500° to 3280° K. The useful range of optical depths for the absorption measurements generally will limit their use to small-scale or low-density experiments. This limitation must be determined for the particular experiment and the choice of wavelength.

Lewis Research Center
National Aeronautics and Space Administration
Cleveland, Ohio, June 9, 1964

REFERENCES

1. Lewis, J. D., and Harrison, D.: A Study of Combustion and Recombination Reactions During the Nozzle Expansion Process in a Liquid Propellant Rocket Engine. Eighth Symposium (International) on Combustion, The Williams & Wilkins Co., 1962, pp. 366-374.

2. Rubins, P. M., and Rhodes, R. P., Jr.: Shock-Induced Combustion with Oblique Shocks: Comparison of Experiment and Kinetic Calculations. AIAA Jour., vol. 1, Dec. 1963, pp. 2778-2784.

3. Landenberg, R. W., et al.: Physical Measurements in Gas Dynamics and Combustion. Princeton Univ. Press, 1954.

4. Simmons, Frederick S.: Spectroscopic Pyrometry of Gases, Flames and Plasmas. ISA Trans., vol. 2, April 1963, pp. 168-189.

5. Lezberg, Erwin A., and Franciscus, Leo C.: Effects of Exhaust Nozzle Recombination on Hypersonic Ramjet Performance: I - Experimental Measurements. AIAA Jour., vol. 1, Sept. 1963, pp. 2071-2076.

6. Ferriso, C. C.: The Emission of Hot CO_2 and H_2O in Small Rocket Exit Exhaust Gases. Eighth Symposium (International) on Combustion, The Williams & Wilkins Co., 1962, pp. 275-287.

7. Carlson, Donald J.: Experimental Determination of Thermal Lag in Gas-Particle Nozzle Flow. ARS Jour., vol. 32, 1962, pp. 1107-1109.

8. Bauer, S. H., Schott, G. L., and Duff, R. E.: Kinetic Studies of Hydroxyl Radicals in Shock Waves. I - The Decomposition of Water Between 2400° and 3200° K. J. Chem. Phys., vol. 28, June 1958, pp. 1089-1096.

9. Penzias, Gunther J., and Maclay, G. J.: Analysis of High Temperature Gases in Situ by Means of Infrared Band Models. NASA CR-54002, W&S TR-28 - Final report on NAS3-1542 - phase III, Dec. 1963.

10. Strong, H. M., and Bundy, F. P.: Measurement of Temperatures in Flames of Complex Structure by Resonance Line Radiation. J. Appl. Phys., vol. 25, 1954, pp. 1521-1537.

11. Buchele, Donald: A Self-Balancing Line-Reversal Pyrometer. In: Temperature, Its Measurement and Control in Science and Industry. Reinhold Pub. Corp., 1962, vol. III, pt. 2, pp. 879-887.

12. Gaydon, A. G., and Hurle, I. R.: Measurement of Times of Vibrational Relaxation and Dissociation Behind Shock Waves in N_2, O_2, Air, CO, CO_2 and H_2. Eighth Symposium (International) on Combustion, The Williams & Wilkins Co., 1962, pp. 309-318.

13. Glawe, George E., Johnson, Robert C., and Krause, Lloyd N.: Intercomparison of Several Pyrometers in a High-Temperature Gas Stream. In: Temperature, Its Measurement and Control in Science and Industry. Reinhold Pub. Corp., 1962, vol. III, pt. 2, pp. 601-605.

14. Buchele, D.: Nonlinear-Averaging Errors in Radiation Pyrometry. NASA TN D-2406, 1964.

15. Oldenberg, O., and Rieke, F. F.: Kinetics of OH Radicals as Determined by Their Absorption Spectrum III. A Quantitative Test for Free OH; Probabilities of Transition. J. Chem. Phys., vol. 6, Aug. 1938, pp. 439-446.

16. Kaskan, W. E.: Hydroxyl Concentration in Rich Hydrogen-Air Flames Held on Porous Burners. Combustion and Flame, vol. 2, Sept. 1958, pp. 229-243.

17. Carrington, Tucker: Line Shape and f Value in the OH $^2\Sigma^+ - {}^2\Pi$ Transition. J. Chem. Phys., vol. 31, 1959, pp. 1243-1252.

18. Dyne, P. J.: Uncertainties in the Measurement of the Oscillator Strength of the Ultraviolet Bands of OH. J. Chem. Phys., vol. 28, May 1958, pp. 999-1001. (See also Tech. Rep. 12, Guggenheim Jet Prop. Center, C.I.T., 1954.)

19. Lapp, M.: Shock-Tube Measurements of the f-Number for the (0,0)-Band of the OH $^2\Sigma \rightarrow {}^2\Pi$ Transitions. C.I.T. Tech. Note no. 11, AF 18(603)-2, May 1960.

20. Dieke, G. H., and Crosswhite, H. M.: The Ultraviolet Bands of OH. Bumblebee Rep. 87, Johns Hopkins Univ., 1948.

21. Learner, R. C. M.: The Influence of Vibration-Rotation Interaction on Intensities of the Electronic Spectra of Diatomic Molecules. I. The Hydroxyl Radical. Proc. Roy. Soc. (London), ser. A, 269, no. 1338, Sept. 1962, pp. 311-326.

22. Kaskan, Walter E.: Line Widths and Integrated Absorption Coefficients for the Ultraviolet Bands of OH. J. Chem. Phys., vol. 29, 1958, pp. 1420-1421.

23. Penner, S. S.: Quantitative Molecular Spectroscopy and Gas Emissivities. Addison-Wesley Pub. Co., Inc., 1959, p. 46.

24. Bennett, R. G., and Dalby, F. W.: Experimental Determination of the Oscillator Strength of the Violet System of OH. J. Chem. Phys., vol. 40, 1964, pp. 1414-1416.

25. Golden, D. M., Del Greco, F. P., and Kaufman, F.: Experimental Oscillator Strength of OH, $^2\Sigma^+ \rightarrow {}^2\Pi$, by a Chemical Method. J. Chem. Phys., vol. 39, 1964, pp. 3034-3041.

26. Zeleznik, Frank J., and Gordon, Sanford: A General IBM 704 or 7090 Computer Program for Computation of Chemical Equilibrium Compositions, Rocket Performance and Chapman-Jouguet Detonations. NASA TN D-1454, 1962.

27. Westenberg, A. A.: Hydrogen-Air Chemical Kinetic Calculations in Supersonic Flow. John Hopkins Univ. Applied Physics Lab. CM-1028, Dec. 1962.

28. Mitchell, A. C. G., and Zemansky, M. W.: Resonance Radiation and Excited Atoms. Cambridge Univ. Press, 1961, p. 325.

29. Penzias, G. J., and Tourin, R. H.: Methods for Infrared Analysis of Rocket Flames in Situ. Combustion and Flame, vol. 6, 1962, pp. 147-152.

30. Oppenheim, U. P., and Ben-Aryeh, Y.: Statistical Model Applied to the Region of ν_3 Fundamental of CO_2 at 1200° K. J. Opt. Soc. Am., vol. 53, March 1962, pp. 344-350.

31. Plass, Gilbert N.: Models for Spectral Band Absorption. J. Opt. Soc. Am., vol. 48, 1958, pp. 690-703.

32. Penzias, G. J.: Spectroscopic Determination of CO_2 Concentration in Situ. Paper presented at Tenth Symposium (International) on Combustion, Cambridge (England), Aug. 17-21, 1964.

33. Bauer, S. H., Kiefer, John H., and Loader, Brian E.: A Study of the Emission Intensities of Cr Lines from Shocked Gases Containing $Cr(CO)_6$. Canadian J. Chem., vol. 39, 1961, pp. 1113-1130.

34. Faizullov, F. S., Sobolev, N. N., and Kudryavtsev, E. M.: Spectroscopic Investigation of the State of the Gas Behind a Shock Wave, II. Optics and Spectroscopy, vol. 8, May 1960, pp. 311-315.

"The aeronautical and space activities of the United States shall be conducted so as to contribute . . . to the expansion of human knowledge of phenomena in the atmosphere and space. The Administration shall provide for the widest practicable and appropriate dissemination of information concerning its activities and the results thereof."

—NATIONAL AERONAUTICS AND SPACE ACT OF 1958

NASA SCIENTIFIC AND TECHNICAL PUBLICATIONS

TECHNICAL REPORTS: Scientific and technical information considered important, complete, and a lasting contribution to existing knowledge.

TECHNICAL NOTES: Information less broad in scope but nevertheless of importance as a contribution to existing knowledge.

TECHNICAL MEMORANDUMS: Information receiving limited distribution because of preliminary data, security classification, or other reasons.

CONTRACTOR REPORTS: Technical information generated in connection with a NASA contract or grant and released under NASA auspices.

TECHNICAL TRANSLATIONS: Information published in a foreign language considered to merit NASA distribution in English.

TECHNICAL REPRINTS: Information derived from NASA activities and initially published in the form of journal articles.

SPECIAL PUBLICATIONS: Information derived from or of value to NASA activities but not necessarily reporting the results of individual NASA-programmed scientific efforts. Publications include conference proceedings, monographs, data compilations, handbooks, sourcebooks, and special bibliographies.

Details on the availability of these publications may be obtained from:

SCIENTIFIC AND TECHNICAL INFORMATION DIVISION

NATIONAL AERONAUTICS AND SPACE ADMINISTRATION

Washington, D.C. 20546